High-Pressure Study of the Local Dynamics of Melt *cis*-1,4-Polybutadiene and *cis*-1,4-Polyisoprene

A. Kirpatch and D. B. Adolf*

Department of Physics and Astronomy, University of Leeds, Leeds, LS2 9JT United Kingdom

Received September 3, 2003; Revised Manuscript Received December 5, 2003

ABSTRACT: Time-resolved optical spectroscopy has been employed to study the local melt segmental dynamics of anthracene-labeled *cis*-1,4-polybutadiene (PB) as a function of pressure (0.1−150 MPa) over a temperature range of 303−323 K. PB activation volumes calculated at fixed temperatures were observed to be independent of pressure but dependent on temperature. PB activation energies calculated at fixed pressures were observed to be independent of temperature but dependent on pressure. These results are qualitatively similar to previously reported findings for *cis*-1,4-polyisoprene (PI). The high-pressure dynamics of PB and PI are shown to be well described by an empirical function of pressure and temperature. An average dT/dP value of 0.15 K MPa^{-1} for PB is calculated and is observed to be significantly temperature and pressure dependent. The ratio of the activation energy at constant volume to the activation energy at constant pressure, Q_V/Q_P, increases from 0.76 to 0.91 as the PB density is increased from 0.88 to 0.94 g cm^{-3} via variations in temperature and pressure.

I. Introduction

Efforts addressing macromolecular structure−property relationships have often approached this line of study through the polymer's local segmental dynamics. These motions occur on the length scale of a few repeat units and hence are heavily influenced by the chemical structure of the repeat unit. These motions are also related to longer length viscoelastic relaxations associated with mechanical polymer properties. These short length scale motions have been experimentally monitored in the solution state and the blended and unblended melt states using a host of experimental techniques including NMR[1−3] dielectric relaxation[4−7] and time-resolved optical spectroscopy (TROS).[8−10] Experiments have been performed as a function of a variety of quantities such as temperature, solvent identity, and solvent quality. However, until recently, little or no effort had been invested into addressing the pressure variable. Following on from the authors' earlier papers dealing with the high-pressure study of the solution state dynamics of *cis*-1,4-polyisoprene (PI)[11] and *cis*-1,4-polybutadiene (PB)[12] in addition to a similar study of melt PI,[13] this paper concentrates on the high-pressure behavior of the local segmental dynamics of melt PB. Activation volumes are observed to be temperature dependent and activation energies pressure dependent in line with observations from earlier studies of PI. dT/dP and Q_V/Q_P values are determined for PB and compared to similar quantities for PI determined by the same technique. Both quantities are observed to be significantly dependent on pressure and temperature. Experimental details now follow in section II. Results and discussion are located within section III with conclusions presented in section IV.

II. Experimental Section

A. Materials and Sample Preparation. Unlabeled PB was purchased from Scientific Polymer Products, Inc., and from Polymer Standards Service. Anthracene center labeled *cis*-1,4-polybutadiene (PB*) used in this study was purchased from Polymer Source, Inc., Québec, Canada. Physical characteristics are given in Table 1 along with molecular weight and polydispersity determined via size exclusion chromatography and microstructures found via ^{13}C NMR. Each polymer chain contains one anthracene chromophore located at the midpoint of the chain. The chain is covalently bonded to the anthracene across the chromophore's 9- and 10-positions, allowing its $S_0 \rightarrow S_1$ electronic transition dipole moment to be oriented along the chain backbone. Local polymer dynamics are monitored through changes in the spatial orientation of this transition dipole as discussed further in the following sections.

PB melt samples doped with PB* were prepared by solvent-casting using toluene (Aldrich, >99.5% purity). Measurements were performed using the M_w = 143K unlabeled PB sample listed in Table 1 with the M_w = 94K unlabeled PB sample listed in Table 1 used only for a few reproducibility checks. The content of labeled polymer corresponded to that required for an optical density of less than 0.1 in a 5 mm path length of melt sample. At least three freeze−pump−thaw cycles were applied to the casting solution to replace molecular oxygen with molecular nitrogen. The solution was then drip-cast into a Teflon former while under a nitrogen atmosphere. Repeated applications were made to build up a sample 2−3 mm in thickness. Once all the visible solvent had evaporated into the nitrogen atmosphere, the last traces of toluene were removed by leaving the sample under vacuum for at least 6 weeks.

B. High-Pressure Cell and Melt Sample Adapter. Details of the high-pressure cell and adapter have been described in previous papers.[11−13] This paper reports data taken at temperatures ranging from 303 to 323 K and at pressures ranging from 0.1 to 150 MPa.

C. Experimental Technique and Data Fitting. Both the time-resolved optical spectroscopy technique[11−13] and associated equipment[10] employed in this study have been described in detail elsewhere. To summarize, the measurement is sensitive to a time-dependent anisotropy, $r(t)$, calculated from the vertical and horizontal fluorescence emission decays, $I_{\parallel}(t)$, and $I_{\perp}(t)$, via

$$r(t) = \frac{I_{\parallel}(t) - I_{\perp}(t)}{I_{\parallel}(t) + 2I_{\perp}(t)} \quad (1)$$

The anisotropy decays were fit to an empirical biexponential function with fitting parameters A, B, τ_1, and τ_2.

$$r(t) = A \exp(-t/\tau_1) + B \exp(-t/\tau_2) \quad (2)$$

* To whom correspondence should be addressed: Tel 0113 3433812; Fax 0113 3433846; e-mail D.B.Adolf@leeds.ac.uk.

10.1021/ma0304630 CCC: $27.50
Published on Web 01/17/2004

Table 1. Physical Characteristics of the Polymers Used in This Study

polymer	$M_w \times 10^{-3}$ (Da)	polydispersity	microstructure			abbrev
			% cis-1,4	% vinyl-1,2	% trans-1,4	
labeled *cis*-1,4-polybutadiene	117	1.05	92	4	4	PB*
unlabeled *cis*-1,4-polybutadiene	143	1.02	98.5	1.1	0.4	PB
unlabeled *cis*-1,4-polybutadiene	94	1.02	86	6	8	PB

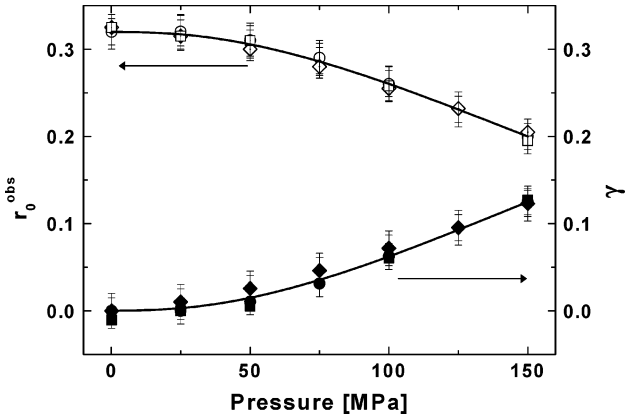

Figure 1. Observed fundamental anisotropy (open symbols) and the scrambling factor (closed symbols) as functions of pressure. Symbols represent melt PB data obtained at different temperatures: 303 K (circles), 313 K (diamonds), and 323 K (squares). Solid lines are third-degree polynomial fits to the data, and the best fit coefficients are reported in Table 2.

Distortions in the data introduced by the finite width of the laser pulse (∼5 ps) and the response of the detection equipment were deconvolved via iterative impulse reconvolution.[14] Reduced χ^2 values for these fits were typically no larger than 1.15. The biexponential fits are used solely to characterize the shape of the anisotropy decays, and no further significance is given to the fit parameters. An average correlation time, τ_c, representing the overall time scale of the monitored segmental dynamic was determined using

$$\tau_c = \frac{1}{r_0}\int_0^\infty r(t)\,dt \tag{3}$$

where r_0 is the fundamental anisotropy and τ_c values are determined via integration of the biexponential fits. Measurements at atmospheric pressure yielded r_0 values for PB* in the range 0.32 ± 0.02, in good agreement with values for other anthracene-labeled PB solutions.[12] Additionally, all reported τ_c values within this paper have an associated error of ±10%.

D. Correction of Pressure-Induced Birefringence. Undesired polarization scrambling is present within the experiment due to the pressure-induced birefringence of the quartz windows. Contributions of this effect to $I_{\parallel}(t)$ and $I_{\perp}(t)$ are corrected for via the method of Paladini and Weber.[15] The scrambling correction factor, γ, is determined at a pressure P as

$$\gamma(P) = \frac{1 - (r_0^{obs}(P)/r_0(P_{atm}))}{3} \tag{4a}$$

where $r_0^{obs}(P)$ is observed value of the fundamental anisotropy at a pressure P and $r_0(P_{atm})$ is the fundamental anisotropy at atmospheric pressure, P_{atm}. In general, the birefringence corrected anisotropy, $r(t)$, is related to the observed anisotropy, $r^{obs}(t)$, through the expression[11]

$$r(t) = r^{obs}(t)\left[\frac{1}{1 - 3\gamma}\right] \tag{4b}$$

Figure 1 reveals γ and r_0^{obs} values as functions of pressure for PB at different temperatures. The solid curves running through the data are third-degree polynomial fits with fit parameters reported in Table 2. As can be seen, r_0^{obs} decreases to no less than 0.2 over the experimental range of pressure, and corrected r_0^{obs} values fall within a window of 0.33 ± 0.02 for all values of temperature and pressure employed within this study.

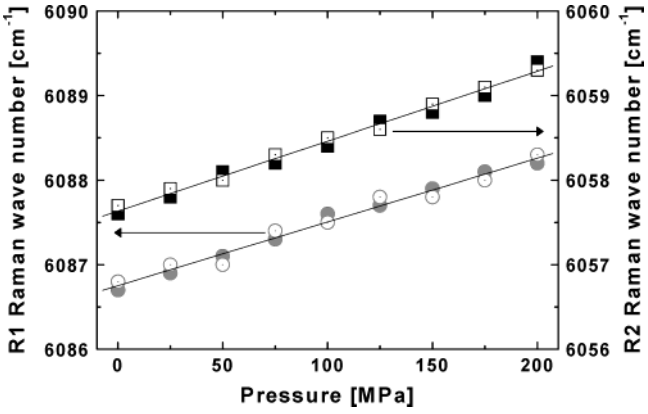

Figure 2. Pressure shift of the ruby R_1 (circles) and R_2 (squares) fluorescence lines. Closed symbols represent a pressurization of the system and open symbols a depressurization. The error bars are less than symbol size.

Table 2. Parameters of Third-Order Polynomial Fits to the Scrambling Factor $\gamma(P)$ and Observed Fundamental Anisotropy $r_0^{obs}(P)$

	A_0	A_1 (MPa^{-1})	A_2 (MPa^{-2})	A_3 (MPa^{-3})
$\gamma(P)$	0.00	-5.07×10^{-5}	9.79×10^{-6}	-2.51×10^{-8}
$r_0^{obs}(P)$	0.32	2.97×10^{-5}	-8.74×10^{-6}	2.06×10^{-8}

E. Pressure Dependence of Ruby Fluorescence Doublet. The pressure dependence of ruby fluorescence was employed to help assess the extent to which the entire melt PB sample was reaching the desired pressure. This approach has previously been employed in the calibration of diamond window pressure cells[16−18] over larger pressure ranges (up to 2300 MPa) than that covered here (up to 150 MPa). The ruby fluorescence shift in a melt sample was detected at high pressure using a PB sample doped with a trace amount of ruby dust. The fluorescence was measured on a Renishaw 2000 Raman imaging system (relative resolution 0.2 cm^{-1}). Figure 2 depicts the observed R_1-line and R_2-line shifts as a function of the pressure read from the gauge attached to the hand pump. Closed symbols represent a pressurization of the system and open symbols a depressurization of the system. Best fit lines are drawn through the two data sets with the slope of each line denoted as $\delta\nu/\delta P$. These measurements yield $\delta\nu/\delta P = 0.0075 \pm 0.0002$ cm^{-1} MPa^{-1} for R_1 and $\delta\nu/\delta P = 0.0083 \pm 0.0002$ cm^{-1} MPa^{-1} for R_2. These values are in good agreement with those (0.0077 and 0.0084 cm^{-1} MPa^{-1}, respectively) obtained by other efforts.[19−21]

III. Results and Discussion

A. Comparison of Atmospheric Pressure Data to Previous Efforts. Melt PB data at atmospheric pressure are plotted in Figure 3. Closed circles correspond to the current data whereas open circles correspond to TROS data obtained by Viovy et al.[22] for bulk PB with a predominately trans microstructure (i.e., 51%). Excellent agreement between two sets of data is observed. The indicated best fit line is associated with the Viovy

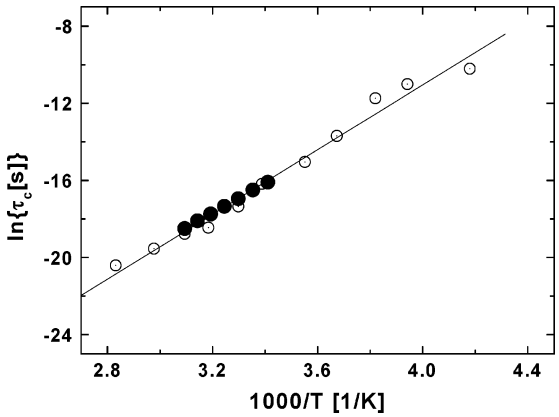

Figure 3. Temperature dependence of the correlation time for PB* in melt PB plotted in Arrhenius format at atmospheric pressure. Data shown are the current work (closed circles) and data from Viovy et al.[22] (open circles). The error bars of the current data are symbol size.

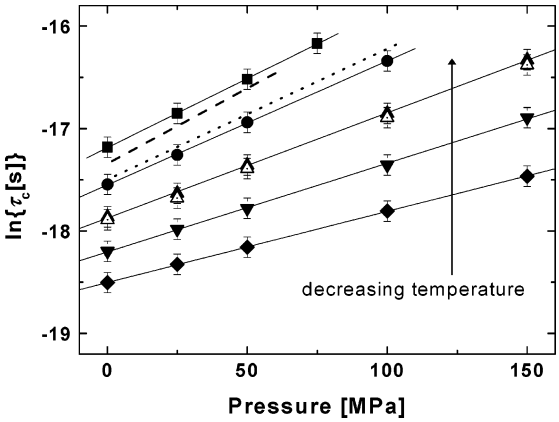

Figure 4. Pressure dependence of PB correlation times at 303 K (squares), 308 K (circles), 313 K (triangles), 318 K (inverted triangles), and 323 K (diamonds). Open symbols correspond to measurements using a second sample performed for reproducibility checks. The dashed line corresponds to PI data at 318 K with the dotted line corresponding to PI at 323 K (see text).

data set but is an equally good fit for the current data and affords an activation energy of 53 kJ mol^{-1} at ambient pressure.

B. Activation Volumes and Activation Energies. Activation volumes (ΔV) associated with PB local dynamics were determined at every temperature under study (i.e., at 303, 308, 313, 318, and 323 K) from the best fit slopes of plots of ln τ_c vs pressure as illustrated in Figure 4. PI data[13] at 318 and 323 K are also included within Figure 4. For clarity, only the best fit lines through these data points are illustrated. Open symbols within this figure represent the data obtained on an additional PB sample for reproducibility checks. It is immediately observed that all ln τ_c vs pressure data for PB are linear over the studied pressures and temperatures as also was observed for PI. PB activation volumes (ΔV) are reported in Table 3 and are observed to decrease with increasing temperature. The same tendency was observed in the authors' previous efforts on PI with ΔV values for PI being slightly more sensitive to temperature than those for PB.

This observed behavior is also in qualitative agreement with findings from other high-pressure investigations of local polymer dynamics.[23] For example, Floudas et al.[4,5] performed dielectric relaxation measurements

Table 3. Activation Volumes ΔV (cm^3 mol^{-1}) of Bulk *cis*-1,4-Polybutadiene Determined from the Slopes of Figure 4[a]

T (K)	measured ΔV	T (K)	measured ΔV
303	35	318	23
308	31	323	19
313	27		

[a] There is an error of ±10% associated with each value.

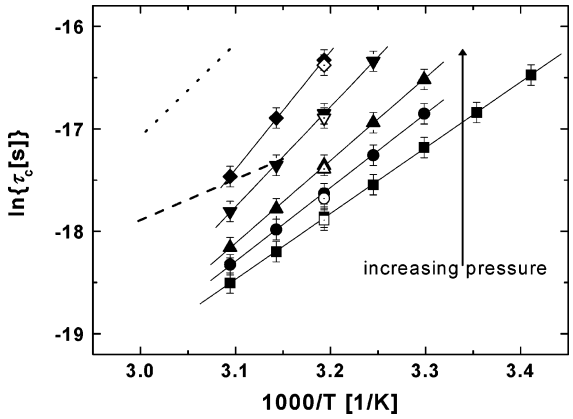

Figure 5. Temperature dependence (i.e., Arrhenius format) of PB correlation times at 0.1 MPa (squares), 25 MPa (circles), 50 MPa (triangles), 100 MPa (inverted triangles), and 150 MPa (diamonds). Open symbols correspond to measurements using a second sample performed for reproducibility checks. The dashed line corresponds to PI at 0.1 MPa, and the dotted line corresponds to PI at 100 MPa (see text).

Table 4. Measured and Calculated Arrhenius Activation Energies Q_P (kJ mol^{-1}) of Bulk *cis*-1,4-Polybutadiene for Each Pressure under Study[a]

pressure (MPa)	measured Q_P	calculated Q_P via eq 5
0.1	53	53
25	60	60
50	67	67
100	81	81
150	96	95

[a] There is an error of ±10% associated with each value.

using PI and a pressure range of 0.1−300 MPa. Samples employed had molecular weights of 1200−26 000 Da with the calculated activation energies decreasing from 95 to 50 cm^3 mol^{-1} over a temperature range of 273−306 K. Temperature-dependent activation volumes have also been reported within computational studies of the high-pressure dynamics of melt polyethylene.[24−26]

Values of the observed activation energies at constant pressure (Q_P) are determined from the slopes of the ln τ_c vs 1000/T plots as shown within Figure 5 at various pressures. Open symbols again correspond to a second sample performed for reproducibility checks and PI data (i.e., dashed line 0.1 MPa and dotted line 100 MPa) is represented as best fit lines only for clarity. The PB data are observed to be well approximated as a linear function of reciprocal temperature with the corresponding Q_P values reported in Table 4. Q_P is observed to be smallest at atmospheric pressure and significantly increases with pressure. The average value of dQ_P/dP is 0.28 kJ mol^{-1} MPa^{-1}. Similar behavior was observed for the authors' measurements of PI where Q_P values increased from 32 to 75 kJ mol^{-1} as pressure increased from 0.1 to 100 MPa, thereby affording an average dQ_P/dP of 0.43 kJ mol^{-1} MPa^{-1}. The observed pressure dependence of PB's Q_P is consistent with the tempera-

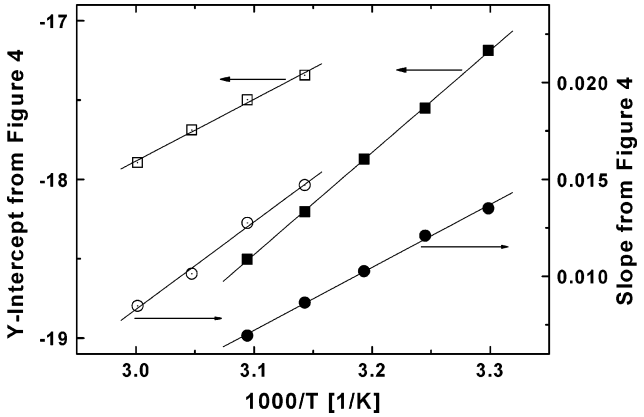

Figure 6. *Y*-intercepts (squares) and slopes (circles) from Figure 4 vs 1000/*T* for PB (closed symbols) and PI (opened symbols). PI data taken from plots similar to Figure 4 as found within a previous publication.[13]

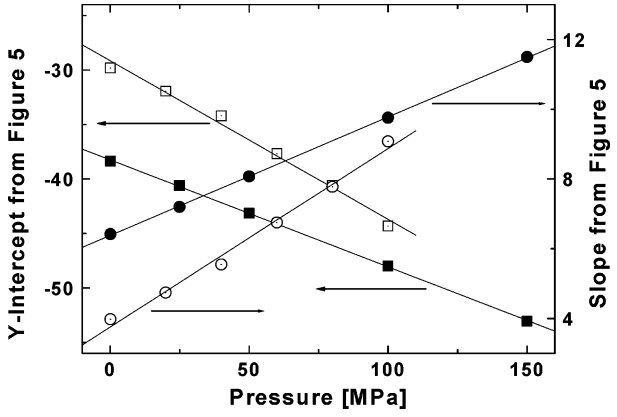

Figure 7. *Y*-intercepts (squares) and slopes (cycles) from Figure 5 vs pressure for PB (closed symbols) and PI (opened symbols). PI data taken from plots similar to Figure 5 as found within a previous publication.[13]

ture dependence of its ΔV values within experimental error through eq 5,[27] as reported in Table 4.

$$Q_P(T,P) = Q_P(T,P=0) + P[\Delta V - T(\mathrm{d}\Delta V/\mathrm{d}T)_P] \quad (5)$$

Pressure-dependent activation energies have also been reported for other polymers.[23] For example, poly(vinyl chloride)[27] Q_P values determined via high-pressure dielectric relaxation from 296 to 353 K were Arrhenius in nature and increased from 50 to 60 kJ mol^{-1} over the pressure range of 0.1−300 MPa. Pressure-dependent activation energies have been reported within computational studies of melt polyethylene.[24−26]

C. *T* and *P* Generalization of ln τ_c, ΔV, and Q_P. The question arises as to whether a single empirical expression can be found to describe accurately both the temperature and pressure dependence of melt PB and PI dynamics. Fitting the data once to such an expression would facilitate further analysis of the data in terms of equations derived from the empirical expression rather than through the use of excessive data interpolation which can compound error. For PB, this expression must account for the observed temperature dependence of the slopes and intercepts of the best fit lines within Figure 4 and the pressure dependence of these same quantities within Figure 5. Similar requirements must be met for PI as found within the authors' aforementioned publication. Figure 6 reveals the temperature dependence of the intercepts and slopes for PI and PB from ln τ_c vs pressure plots is well described as linear functions of reciprocal temperature. This suggests

$$\ln \tau_c = A(T) + B(T)P \quad (6)$$

where

$$A(T) = a_1 + a_2(1/T)$$

and

$$B(T) = b_1 + b_2(1/T)$$

Substitution offers the general equation

$$\ln \tau_c = a_1 + a_2(1/T) + [b_1 + b_2(1/T)]P \quad (7)$$

Similarly, Figure 7 reveals the pressure dependence of the intercepts and slopes for PI and PB from ln τ_c vs 1000/*T* plots is well described as a linear function of pressure. This suggests

$$\ln \tau_c = C(P) + D(P)(1/T) \quad (8)$$

where

$$C(P) = c_1 + c_2P$$

and

$$D(P) = d_1 + d_2P$$

Substitution again offers the general equation

$$\ln \tau_c = c_1 + c_2P + (d_1 + d_2P)(1/T) \quad (9)$$

As eqs 7 and 9 are derived from the same data set, it is clear that $a_1 = c_1 = \alpha$, $c_2 = b_1 = \beta$, $a_2 = d_1 = \gamma$, and $b_2 = d_2 = \omega$, suggesting the general expression

$$\ln \tau_c = \alpha + \beta P + \gamma(1/T) + \omega P/T \quad (10)$$

where the parameters α, β, γ, and ω are not pressure dependent.

Table 5. Best-Fit Parameters of Eq 10 Describing the (ln τ_c, *P*, *T*) Landscapes for *cis*-1,4-Polybutadiene and *cis*-1,4-Polyisoprene Using τ_c (in seconds)

	α	β (MPa^{-1})	$\gamma \times 10^{-3}$ (K)	$\omega \times 10^{-3}$ (K MPa^{-1})
cis-1,4-polybutadiene	−38.3	−0.096	6.41	0.0332
cis-1,4-polyisoprene	−29.4	−0.136	3.83	0.0482

Best-fit values for α, β, γ, and ω for PB and PI are reported in Table 5. These coefficients are observed (not shown) to reproduce the experimentally determined τ_c values to within 5% in all cases and to within 3% in most cases. Activation volumes and activation energies are expressed through α, β, γ, and ω as

$$\Delta V = R(\beta T + \omega) \quad (11)$$

and

$$Q_P = R(\gamma + \omega P) \quad (12)$$

where *R* is the universal gas constant.

D. Slices of the (ln τ_c, *P*, *T*) Surface at Fixed Values of ln τ_c. The (ln τ_c, *P*, *T*) surface described by eq 10 can be fully appreciated by slicing it along the

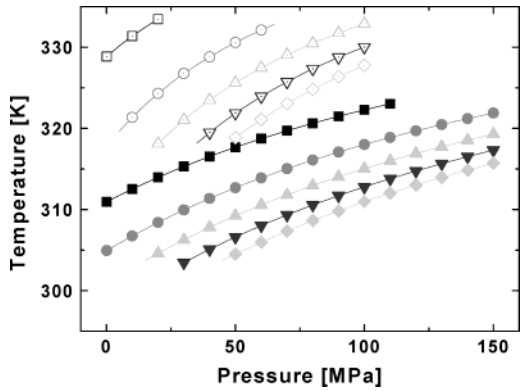

Figure 8. Pressure and temperature cross plots corresponding to PB relaxation data at τ_c values of 20 ns (squares), 30 ns (circles), 40 ns (triangles), 50 ns (inverted triangles), and 60 ns (diamonds). Closed symbols correspond to PB whereas opened symbols represent PI data taken from a previous study.[13] Lines connecting data points are an aid to the eye.

different axes. Figure 4 represents ln τ_c, P slices at various fixed values of temperature, whereas Figure 5 represents ln τ_c, T slices (n.b. plotted with a 1000/T axis) at several fixed values of pressure. This leaves the P, T slices to be plotted at fixed ln τ_c values as shown in Figure 8 for PB and PI. These slices are plotted as T vs P to give a clearer picture of the behavior of the slope, $(dT/dP)_{\tau_c}$. The steadily increasing nature of the curves in Figure 8 is due to the fact that that faster dynamics occur at higher temperatures at fixed pressures and lower pressures at fixed temperatures. The unequal spacing between the lines at each of the different ln τ_c values for PB and PI is due to the pressure-dependent nature of the activation energies and the temperature-dependent nature of the activation volumes. Lines corresponding to PI data are steeper than those corresponding to PB data. This is consistent with PI's increased sensitivity to pressure as observed within Figure 5. The nature of these lines implies $(dT/dP)_{\tau_c}$ values are not constant and depend on temperature and pressure which is discussed in greater detail within the next section.

E. $(dT/dP)_{\tau_c}$ Values. The pressure and temperature dependence of the local dynamics allows $(dT/dP)_{\tau_c}$ (hereafter denoted within the text as dT/dP) to be determined through the activation volumes and activation energies via the expression[28]

$$\left(\frac{dT}{dP}\right)_{\tau_c} = \frac{T\Delta V}{Q_P} \tag{13}$$

This expression should not be confused with the description of the solid−liquid boundary in phase diagrams as described by the Clapeyron equation

$$\left(\frac{dT}{dP}\right)_{\Delta G} = \frac{T\Delta V}{\Delta H}$$

where ΔH is the enthalpy of fusion and ΔV is the volume change on melting.

A shortcoming of eq 13 is how it indirectly masks the pressure and temperature dependence imparted to dT/dP through ΔV and Q_P. This dependence can be made more obvious by using eqs 11 and 12 to derive an expression for dT/dP where the effective pressure and temperature dependence is explicitly present. For the

Table 6. dT/dP Values Calculated from Eq 14 for Each Temperature and Pressure Studied[a]

	dT/dP (K MPa^{-1})				
press. [MPa]	303 K	308 K	313 K	318 K	323 K
0.1	0.20 (34)	0.18 (24)	0.16 (17)	0.14 (13)	0.11 (9)
25	0.17 (48)	0.16 (32)	0.14 (22)	0.12 (16)	0.10 (11)
50	0.16 (67)	0.14 (44)	0.12 (29)	0.11 (19)	0.09 (13)
100		0.12 (80)	0.10 (48)	0.09 (30)	0.07 (18)
150			0.08 (80)	0.08 (45)	0.06 (26)

[a] The correlation time of the local dynamics in nanoseconds at each pressure and temperature is indicated in parentheses after each value of dT/dP.

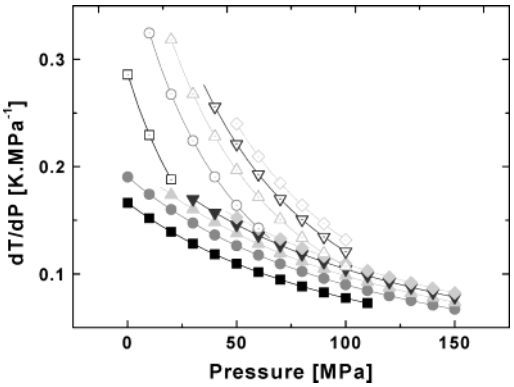

Figure 9. dT/dP vs pressure for fixed τ_c of 20 ns (squares), 30 ns (circles), 40 ns (triangles), 50 ns (inverted triangles), and 60 ns (diamonds). Closed symbols correspond to PB, whereas open symbols represent PI data taken from a previous publication.[13] Lines connecting data points are an aid to the eye.

(ln τ_c, P, T) surface within this paper, this expression is

$$\left(\frac{dT}{dP}\right)_{\tau_c} = \frac{T(\beta T + \omega)}{\gamma + \omega P} \tag{14}$$

Values for PB using eq 14 are reported in Table 6 along with the correlation time of the dynamics at the indicated pressure and temperature. The dT/dP value for PB averaged over all temperatures and pressures within this study is 0.15 K MPa^{-1}, whereas for PI this average is 0.20 K MPa^{-1}. Both of these values are in good agreement with Ferry,[29] who cites the magnitude is generally 0.20 ± 0.05 K MPa^{-1} based on bulk viscoelasticity measurements for a number of polymers. Frick et al. performed high-pressure incoherent inelastic neutron scattering measurements[30,31] on polybutadiene, which was 52% trans with a molecular weight of 8000 and possessed a T_g of 178 K. Based on pressure-induced line width broadening data, this work revealed values of 0.18 K MPa^{-1}. Frick et al. note that this value is higher than the value of 0.11−0.13 K MPa^{-1} based on the pressure-induced shift of the glass transition temperature determined by calorimetry.

Table 6 reveals that at a fixed temperature the dT/dP values decrease and the τ_c values increase as pressure is increased. At a fixed pressure, both the dT/dP and τ_c values decrease as temperature increases. The pressure dependence of dT/dP of fixed τ_c values is illustrated in Figure 9. Lines connecting data points are given as an aid to the eye. The data within this figures are the slopes of the separate lines shown in Figure 8 and are observed to decrease with pressure at each fixed τ_c value. The PI data are more sensitive to pressure as expected on the basis of data within Figure 4.

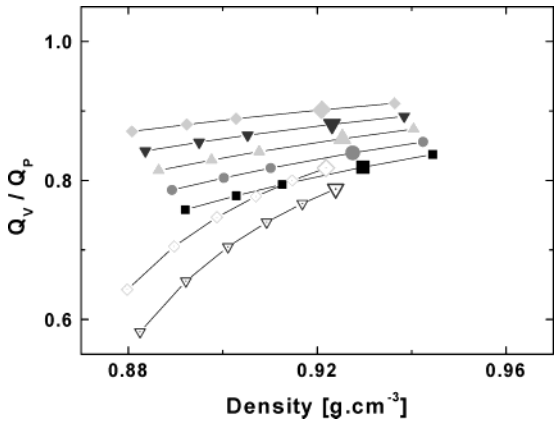

Figure 10. Q_V/Q_P ratio as a function of density for temperatures of 303 K (squares), 308 K (circles), 313 K (triangles), 318 K (inverted triangles), and 323 K (diamonds). Closed symbols correspond to PB, whereas open symbols represent PI data taken from a previous publication.[13] Lines connecting data points are an aid to the eye with the larger symbols representing data taken at 100 MPa.

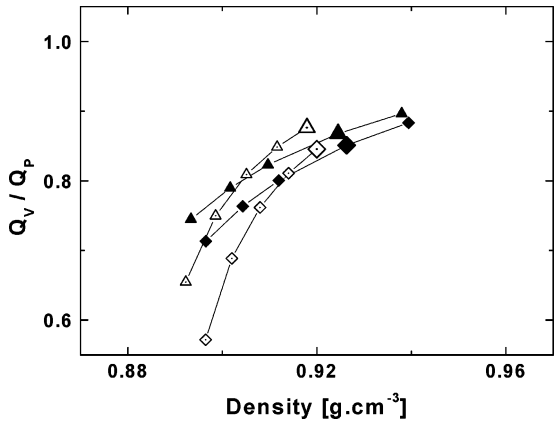

Figure 11. Q_V/Q_P ratio as a function of density for τ_c of 40 ns (triangles) and 60 ns (diamonds). Closed symbols correspond to PB, whereas open symbols represent PI data taken from a previous publication.[13] Lines connecting data points are an aid to the eye with the larger symbols representing data taken at 100 MPa.

F. Density Effects on Q_P and Q_V. Additional insight into Q_P is available through the expression[27]

$$\frac{Q_V(T,V)}{Q_P(T,P)} = 1 - \left(\frac{\mathrm{d}T}{\mathrm{d}P}\right)_{\tau_c}\left(\frac{\mathrm{d}P}{\mathrm{d}T}\right)_V \qquad (15)$$

where Q_V is an activation energy at constant volume. $(\mathrm{d}P/\mathrm{d}T)_V$ is the thermal pressure coefficient and can be expressed as the ratio of the thermal expansivity coefficient, $\alpha(P,T)$, to the isothermal compressibility coefficient, $\kappa(P,T)$. Values of these derivatives have been computed for PB and PI using the PVT data of Yi and Zoller.[32]

The PI samples for the PVT data had a $M_w = 173$K with a polydispersity of 1.38 and a microstructure of 76% cis, 16% trans, and 8% vinyl. The PB samples for the PVT data had a $M_w = 140$K with a polydispersity of 1.13 and a microstructure of 40% cis, 52% trans, and 8% vinyl. $(\mathrm{d}P/\mathrm{d}T)_V$ values for both PB and PI are observed to be pressure and temperature dependent. As pressure is varied from 0.1 to 150 MPa, PB $(\mathrm{d}P/\mathrm{d}T)_V$ values change from 1.32 to 1.46 MPa K^{-1} at 303 K and from 1.24 to 1.39 MPa K^{-1} at 323 K. For PI over this same pressure range, $(\mathrm{d}P/\mathrm{d}T)_V$ values increase from 1.05 to 1.20 MPa K^{-1} at 318 K and from 0.99 to 1.16 MPa K^{-1} at 333 K.

The second term on the right-hand side of eq 15 that involves these derivatives can be interpreted as the fraction of Q_P spent on forming the requisite free volume for the segmental motion to occur, whereas the ratio Q_V/Q_P is the fraction of Q_P spent on the actual activated segmental motion. Figure 10 reveals the density dependence of the Q_V/Q_P ratio for PI and PB. Data at the same temperature are connected by solid lines as an aid to the eye, and $\mathrm{d}T/\mathrm{d}P$ values listed within Table 6 have been employed. Isothermally speaking, Q_V/Q_P values increase with density and are larger at higher temperatures at a fixed density. From an isobaric perspective, this ratio decreases with increasing density. The effect of isothermal densification is more pronounced for PI whereas differences in isobaric densification between the two polymers are not as large. Figure 11 illustrates Q_V/Q_P values determined for fixed correlation times as a function of density where the $\mathrm{d}T/\mathrm{d}P$ values illustrated within Figure 9 are used. These Q_V/Q_P values also are observed to increase with density with higher values of Q_V/Q_P realized for faster dynamics at fixed values of density. As observed previously, PI's Q_V/Q_P values are more sensitive to densification then that for PB.

Overall, Q_V/Q_P values fall within the window of 0.76−0.91 for PB and from 0.57 to 0.88 for PI via variations in temperature and pressure. These ranges are consistent with average Q_V/Q_P ratios determined for other polymers. Values of 0.88 for poly(vinyl chloride),[27] 0.6 for poly(vinyl acetate),[33] and 0.71−0.76 for polyethylene[32] have been reported. Computer simulation of polyethylene performed by Bharadwaj and Boyd[25] provides values of 0.81−0.85. The increase of Q_V/Q_P via isothermal densification and its decrease with isobaric densification have been reported by Williams for poly(methyl acrylate)[27] and for poly(propylene oxide)[27] and by Sayre for polyethylene.[34]

IV. Conclusions

The local dynamics of *cis*-1,4-polybutadiene have been measured over a temperature range of 303−323 K and a pressure range of 0.1−150 MPa via time-resolved optical spectroscopy. Results have been analyzed in terms of activation energies (Q_P) and activation volumes with comparisons drawn to the author's earlier work on the high-pressure local motion of *cis*-1,4-polyisoprene. For both materials, activation energies are Arrhenius though illustrate a significant pressure dependence. Activation volumes in both cases are not dependent on pressure though are dependent on temperature.

Q_P values for both polymers are addressed in terms of a term linked with the availability of free volume and another term linked with the energy required to execute the local motion. The latter term is entitled the constant volume activation energy, Q_V. Within this study, both PB and PI reveal Q_V/Q_P ratios that are consistently above 0.5, in good agreement with other polymers as discussed previously. *cis*-1,4-Polybutadiene ratios were observed on average to be higher than those for *cis*-1,4-polyisoprene values with significant dependence on pressure, temperature, and correlation time observed for this ratio for both of the polydienes studied.

Values of the ratio of Q_V to Q_P which lie between 0.5 and 1.0 indicate Q_V, and hence the thermal demand associated with activated local motion is the dominant contribution to Q_P. Values between 0 and 0.5 would

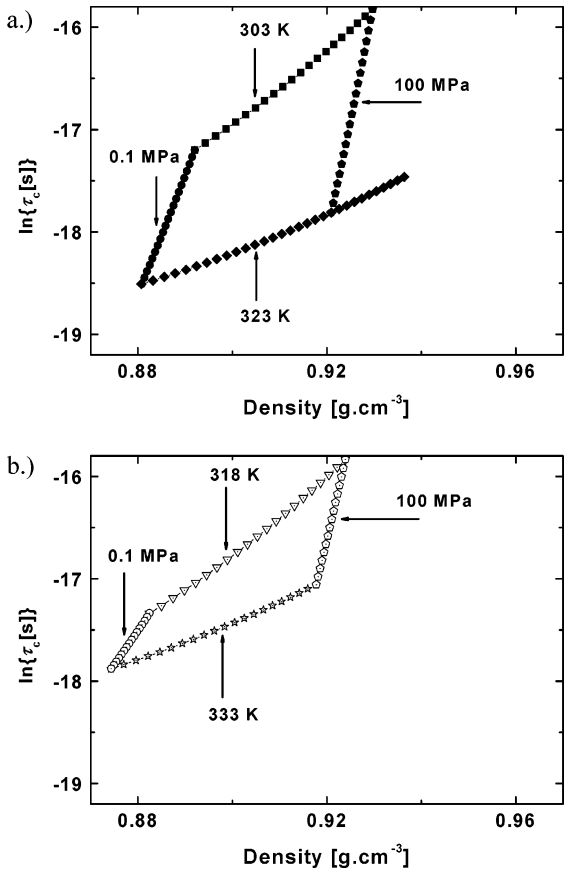

Figure 12. Density dependencies of (a) PB and (b) PI correlation times represented as isotherms at 303 K (squares), 318 K (inverted triangles), 323 K (diamonds), and 333 K (stars) and as isobars at 0.1 (circles) and 100 MPa (pentagons). PI data were taken from a previous publication.[13]

imply the free volume concerns dominated. This is reinforced by Figure 12a,b where the local polymer dynamics are observed to be more sensitive to density changes at fixed pressures rather than at fixed temperatures.

Acknowledgment. The authors are grateful to Graham Williams for valuable discussions concerning high-pressure polymer dynamics. Furthermore, the authors acknowledge funding from the EPSRC (i.e. GR/R17232) and the IRC in Polymer Science and Technology within the Department of Physics and Astronomy at the University of Leeds, UK.

Supporting Information Available: Further discussion of temperature-dependent activation volumes and pressure-dependent activation energies and, additionally, an extension of eq 10 that accounts for curvature in ln τ_c vs 1000/T plots. This material is available free of charge via the Internet at http://pubs.acs.org.

References and Notes

(1) Lauprêtre, F.; Bokobza, L.; Monnerie, L. *Polymer* **1993**, *34*, 468−475.
(2) Chung, G. C.; Kornfield, J. A.; Smith, S. D. *Macromolecules* **1994**, *27*, 5729−5741.
(3) Chung, G. C.; Kornfield, J. A.; Smith, S. D. *Macromolecules* **1994**, *27*, 964−973.
(4) Floudas, G.; Reisinger, T. *J. Chem. Phys.* **1999**, *111*, 5201−5204.
(5) Floudas, G.; Gravalides, C.; Reisinger, T.; Wegner, G. *J. Chem. Phys.* **1999**, *111*, 9847−9852.
(6) Adachi, K.; Imanishi, Y.; Shinkado, T.; Kotaka, T. *Macromolecules* **1989**, *22*, 2391−2395.
(7) Adachi, K. *Macromolecules* **1990**, *23*, 1816−1821.
(8) Hyde, P. D.; Waldow, D. A.; Ediger, M. D.; Kitano, T.; Ito, K. *Macromolecules* **1986**, *19*, 2533−2538.
(9) Hyde, P. D.; Ediger, M. D.; Kitano, T.; Ito, K. *Macromolecules* **1989**, *22*, 2253−2259.
(10) Adams, S.; Adolf, D. B. *Macromolecules* **1998**, *31*, 5794−5799.
(11) Punchard, B. J.; Adolf, D. B. *Macromolecules* **2002**, *35*, 3281−3287.
(12) Punchard, B. J.; Kirpatch, A.; Adolf, D. B. *Polymer* **2002**, 43, 6287−6293.
(13) Punchard, B. J.; Adolf, D. B. *J. Chem. Phys.* **2002**, *117*, 7774−7780.
(14) Birch, D. J. S.; Imhof, R. E. *Topics in Fluorescence Spectroscopy*; Plenum: New York, 1991.
(15) Paladini, A. A.; Weber, G. *Rev. Sci. Instrum.* **1981**, *52*, 419−427.
(16) Dadashev, A.; Pasternak, M. P.; Rozenberg, G. K.; Taylor, R. D. *Rev. Sci. Instrum.* **2001**, *72*, 2633−2637.
(17) Zhao, J.; Hearne, G. R.; Maaza, M.; Laher-Lacour, F.; Witcomb, M. J.; Le Bihan, T.; Mezouar, M. *J. Appl. Phys.* **2001**, *90*, 3280−3285.
(18) Jayasankar, C. K.; Babu, P.; Tröster, Th.; Holzapfel, W. B. *J. Lumin.* **2000**, *91*, 33−39.
(19) Forman, R. A.; Piermarini, G. J.; Barnett, J. D.; Block, S. *Science* **1972**, *176*, 284−285.
(20) Piermarini, G. J.; Block, S.; Barnett, J. D.; Forman, R. A. *J. Appl. Phys.* **1975**, *46*, 2774−2780.
(21) Barnett, J. D.; Block, S.; Piermarini, G. J. *Rev. Sci. Instrum.* **1973**, *44*, 1−9.
(22) Viovy, J.-L.; Monnerie, L.; Merola, F. *Macromolecules* **1985**, *18*, 1130−1137.
(23) Further comparisons found within the Supporting Information for this article.
(24) Bharadwaj, R. K.; Boyd, R. H. *Macromolecules* **2000**, *33*, 5897−5905.
(25) Bharadwaj, R. K.; Boyd, R. H. *J. Chem. Phys.* **2001**, *114*, 5061−5068.
(26) Hotston, S. D.; Adolf, D. B.; Karatasos, K. *J. Chem. Phys.* **2001**, *115*, 2359−2368.
(27) Williams, G. *Trans. Faraday Soc.* **1964**, *60*, 1556−1573. (b) Williams, G. *Trans. Faraday Soc.* **1966**, *62*, 2091−2102. (c) Williams, G. *Trans. Faraday Soc.* **1965**, *61*, 1564−1577. (d) Williams, G. *Trans. Faraday Soc.* **1971**, *67*, 1971−1979.
(28) Williams, G. *Trans. Faraday Soc.* **1964**, *60*, 1548−1555.
(29) Ferry, J. D. *Viscoelastic Properties of Polymers*, 3rd ed.; Wiley: New York, 1980.
(30) Frick, B.; Alba-Simonesko, Ch. *Physica B* **1999**, *266*, 13−19.
(31) Frick, B.; Alba-Simonesko, Ch.; Hendricks, J.; Willner, L. *Prog. Theory Phys. Suppl.* **1997**, *126*, 213−218.
(32) Yi, X. Y.; Zoller, P. *J. Polym. Sci., Part B: Polym. Phys.* **1993**, *31*, 779−788.
(33) Roland, C. M.; Casalini, R. *Macromolecules* **2003**, *36*, 1361−1367.
(34) Sayre, J. A.; Swanson, S. R.; Boyd, R. H. *J. Polym. Sci., Part B: Polym. Phys.* **1978**, *16*, 1739−1759.

MA0304630